Genome-Wide Identification of GRF and GIF Genes in Larix kaempferi and Their Potential Association with Somatic Embryogenesis, Hormone Responses, and miR396-Mediated Regulation

Yuqin Huang
Chinese Academy of Forestry
Ruxin Zhang
Hebei Agricultural University
Xin Li
Northeast Forestry University
Liwang Qi
Chinese Academy of Forestry
Lifeng Zhang
zhanglifeng1029@caf.ac.cn

Chinese Academy of Forestry

Research Article

Keywords: Growth-Regulating Factor (GRF), GRF-Interacting Factor (GIF), Larix kaempferi, Somatic Embryogenesis, miR396

Posted Date: March 30th, 2026

DOI: https://doi.org/10.21203/rs.3.rs-9181763/v1

Additional Declarations: No competing interests reported.

Version of Record: A version of this preprint was published at Plant Cell, Tissue and Organ Culture (PCTOC) on June 4th, 2026. See the published version at https://doi.org/10.1007/s11240-026-03496-x.

Genome-Wide Identification of *GRF* and *GIF* Genes in *Larix kaempferi* and Their Potential Association with Somatic Embryogenesis, Hormone Responses, and miR396-Mediated Regulation

Yuqin Huang[1,2], Ruxin Zhang[3], Xin Li[2], Liwang Qi[1], Lifeng Zhang[1,*]

[1] State Key Laboratory of Tree Genetics and Breeding, Key Laboratory of Tree Breeding and Cultivation of the National Forestry and Grassland Administration, Research Institute of Forestry, Chinese Academy of Forestry, Beijing 100091, China
[2] State Key Laboratory of Tree Genetics and Breeding, Northeast Forestry University, Harbin 150040, China
[3] Hebei Agricultural University, Baoding, 071001, China
* Correspondence: zhanglifeng1029@caf.ac.cn (L.Z.)

Abstract

This study systematically identified and characterized the Growth-regulating factors (*GRFs*) and GRF-interacting factors (*GIFs*) gene families in *Larix kaempferi*, revealing five *LkaGRF* and three *LkaGIF* genes. All LkaGRF proteins contain conserved QLQ and WRC domains, while LkaGIF proteins possess the SSXT domain, confirming their structural conservation across land plants. Phylogenetic analysis placed most LkaGRFs in a gymnosperm-specific clade, indicating ancient lineage diversification, whereas LkaGIFs showed both conserved and gymnosperm-specific branches. Predicted miR396 target sites were detected in all LkaGRF transcripts, and 5′ RLM-RACE further supported miR396-directed cleavage of LkaGRF3 and LkaGRF5. Promoter analysis revealed abundant hormone- and stress-responsive cis-elements. Expression profiling demonstrated that both gene families are significantly upregulated at day 28 during somatic embryogenesis, corresponding to the critical stage of cotyledon differentiation. Hormonal treatments showed that most *LkaGRFs* are rapidly downregulated by IAA, ABA, GA, and SA, *LkaGRF1* showed a generally sustained repressed expression pattern under all five hormone treatments, whereas *LkaGRF3* and *LkaGRF5* were continuously and significantly downregulated by IAA, ABA, GA, and SA. These results support the potential involvement of the miR396-GRF/GIF module in somatic embryogenesis and hormone-responsive developmental processes in *L. kaempferi*, and provide candidate regulators for future functional studies in conifer embryogenic systems.

Keywords: Growth-Regulating Factor (*GRF*); GRF-Interacting Factor (*GIF*); *Larix kaempferi*; Somatic Embryogenesis; miR396

1. Introduction

Larix kaempferi is one of the most important fast-growing plantation tree species in China. Owing to its rapid growth, high wood quality, and strong environmental adaptability, it occupies a central position in sustainable forestry programs(Xu et al. 2021; Qu et al. 2022). However, its long generation

time and complex genetic background severely limit the efficiency of conventional seed propagation and traditional breeding, thereby constraining the rapid fixation and large-scale dissemination of elite traits. Somatic embryogenesis (SE) has emerged as a powerful biotechnological platform for large-scale clonal propagation and genetic transformation of elite conifer genotypes. Since its first establishment in *Picea abies*(Inger et al. 1985) and *Larix decidua*(Nagmani R. and Bonga J. M. 1985), SE has been widely applied in the genus *Larix* and has become an important experimental system for investigating developmental regulation in gymnosperms. Nevertheless, practical application of SE in *L. kaempferi* remains hindered by low embryogenic callus induction rates, frequent embryo abnormalities, and asynchronous development(Filonova et al. 2000; Shmakov and Konstantinov 2020; Zhang et al. 2021b), highlighting the limited understanding of the molecular regulatory networks underlying embryogenic initiation and embryo development in conifers. Previous morphological studies have established a developmental staging framework for *L. kaempferi* somatic embryogenesis(Zhang et al. 2012), providing a basis for examining stage-specific gene expression in this study.

Plant growth and organogenesis are orchestrated by complex transcriptional networks integrating developmental cues, environmental signals, and phytohormone pathways(Yu et al. 2021; Luo and Palmgren 2021). Growth-regulating factors (*GRFs*) are plant-specific transcription factors characterized by two conserved domains, QLQ and WRC, while GRF-interacting factors (*GIFs*) are transcriptional co-activators containing the SSXT domain. GRFs physically interact with GIFs to form GRF–GIF complexes, which have been shown to regulate cell proliferation, organ growth, and meristem activity in angiosperms.(Kim 2019). In angiosperms, the miR396–GRF–GIF regulatory module acts as a central hub controlling organ size, leaf morphogenesis, floral development, root meristem maintenance, and grain yield(Li et al. 2016; Szczygieł-Sommer and Gaj 2019; Liebsch and Palatnik 2020; Lu et al. 2022). Recent studies have further shown that GRFs and GRF–GIF chimeric proteins dramatically enhance in vitro regeneration efficiency across both monocots and dicots, offering a superior alternative to conventional regulators such as BABY BOOM (*BBM*) or WUSCHEL (*WUS*) without causing reproductive abnormalities(Debernardi et al. 2020; Duan et al. 2022; Bull et al. 2023). In addition, *GRF* and *GIF* genes have been associated with multiple phytohormone signaling pathways and stress responses in several angiosperm species(Wang et al. 2020; Iqbal et al. 2022; Fu et al. 2024; Alongi et al. 2025). These findings highlight the potential importance of this regulatory module in developmental reprogramming and biotechnological applications.

miR396 is a conserved upstream regulator of GRF genes and has been widely reported to mediate GRF transcript cleavage in plants. The miR396-GRF module has been associated with organ development, regeneration, and embryogenic processes in several species(Liebsch and Palatnik 2020; Lu et al. 2022; Lee et al. 2022). Our previous work in *L. kaempferi* suggested that miR396 may be involved in somatic embryo regeneration, prompting further investigation of GRF and GIF genes as potential components of this regulatory pathway.

In this study, we performed a genome-wide identification and characterization of *GRF* and *GIF* gene families in *L. kaempferi*. We analyzed their phylogenetic relationships, conserved domains, gene structures, and promoter cis-acting elements, and predicted potential miR396 target sites. We further examined their expression patterns during different stages of somatic embryogenesis and under multiple

hormone treatments. In addition, 5′ RLM-RACE was conducted to validate miR396-directed cleavage of selected *LkaGRF* transcripts. By integrating gene family characterization, developmental expression profiling, hormone responsiveness, and experimental evidence for miR396-mediated targeting, this study aimed to explore the potential involvement of the miR396-GRF/GIF module in somatic embryogenesis and developmental regulation in *L. kaempferi*.

2. Materials and Methods

2.1 Plant Materials and Culture Conditions

The C6 embryogenic cell line of *L. kaempferi*, which exhibits stable somatic embryogenesis (SE) capacity, was used in this study. Immature cones were collected annually in mid-to-late June from trees growing at the Dagujia Forest Farm, Qingyuan County, Liaoning Province, China. This site is the National Long-term Scientific Research Base for Larch Breeding and Cultivation (Northeast China), affiliated with the Research Institute of Forestry, Chinese Academy of Forestry. Immature zygotic embryos were excised and cultured on induction medium at 22 °C in darkness. After embryogenic tissues formed, they were transferred to solid proliferation medium and subcultured every 21 days. The proliferation culture conditions were as previously described by(Zhang et al. 2021a). Cultures were maintained in darkness at 23 °C. Samples were collected after 21 days of subculture, immediately frozen in liquid nitrogen, and stored at −80 °C(Kang et al. 2021).

For somatic embryo development, the C6 line was cultured on solid proliferation medium for 15 days in darkness and then transferred to differentiation medium. The differentiation medium contained 450 mg/L glutamine, 500 mg/L casein hydrolysate, 100 mg/L inositol, 35 g/L sucrose, 4 g/L phytagel, 7.5% (w/v) polyethylene glycol (PEG 4000), and 75 μM abscisic acid (ABA). Cultures were maintained in darkness at 25 ± 2 °C.

2.2 Experimental Treatments and Sample Collection

According to our previous morphological studies, somatic embryo development in *L. kaempferi* can be divided into the following stages: proembryogenic mass (0 d), early single embryo (1-5 d), middle single embryo (5-15 d), late single embryo (15-21 d), early cotyledonary embryo (21-28 d), middle cotyledonary embryo (28-35 d), and mature embryo (35-42 d) (Fan et al. 2020, 2021). Based on this developmental staging system, samples for somatic embryogenesis analysis were collected at key transition time points, namely 0, 2, 5, 10, 15, 21, 28, 35, and 42 d after induction. All samples were immediately frozen in liquid nitrogen and stored at −80 °C until RNA extraction. Three biological replicates were included for each stage(Fan et al. 2020, 2021).

For hormone treatments, embryogenic tissues that had been cultured on solid proliferation medium for 15 d were used as experimental materials. Approximately 2 g of embryogenic tissue were transferred to 250 mL flasks containing 100 mL liquid proliferation medium and cultured at 25 °C in darkness with shaking (100–110 rpm) for 10 days (Zhang et al., 2019b). When the suspension reached approximately 200 mg/mL fresh weight, cultures were divided into five groups and treated with 50 μM salicylic acid (SA), gibberellic acid (GA), ABA, indole-3-acetic acid (IAA), or jasmonic acid (JA). Samples were collected at 0, 3, 6, 9, 12, 24, and 48 h after treatment. The 0

h samples served as the untreated control. All samples were immediately frozen in liquid nitrogen, and stored at −80 °C. Each treatment included three biological replicates(Zhang et al. 2021a).

2.3 Cloning and Identification of *GRF* and *GIF* Genes

Members of the *GRF* and *GIF* gene families in *L. kaempferi* were identified using combined BLASTP and Hidden Markov Model (HMM) approaches. *GRF* and *GIF* protein sequences from *A. thaliana* were retrieved from TAIR and used as reference queries. BLASTP searches against the *L. kaempferi* protein database were conducted with an E-value threshold of 1×10^{-5}.

HMM profiles corresponding to the conserved QLQ (PF08879) and WRC (PF08880) domains of *GRF* proteins and the SSXT domain (PF05030) of *GIF* proteins were downloaded from Pfam. HMMER v3.1 was used to screen the *L. kaempferi* protein database with an E-value cutoff < 0.001. Candidate sequences from BLAST and HMM analyses were integrated and redundant entries removed. Domain validation was performed using InterProScan and the NCBI Conserved Domain Database (CDD). Proteins containing both QLQ and WRC domains were defined as *GRF* members, whereas proteins containing the SSXT domain were classified as *GIF* members.

To confirm sequence accuracy, full-length coding sequences of *LkaGRF* and *LkaGIF* genes were cloned. Total RNA was extracted from embryogenic tissues using the RNAprep Pure Plant Plus Kit (Tiangen). First-strand cDNA was synthesized using the TaKaRa reverse transcription kit. Gene-specific primers (Table S1) were designed using Primer-BLAST and Primer Premier 6.0.

PCR products were verified by 1% agarose gel electrophoresis, purified, and ligated into the pEASY R-Blunt Zero Cloning Vector (TransGen). Recombinant plasmids were transformed into *Escherichia coli* Trans1-T1 competent cells. Positive clones were screened by colony PCR and sequenced (Genewiz, Suzhou, China). Sequencing results were aligned with predicted sequences for validation.

2.4 Sequence Alignment and Phylogenetic Analysis

Multiple sequence alignment of *LkaGRF* and *LkaGIF* proteins was performed using ClustalW implemented in MEGA X. Conserved domains (QLQ, WRC, and SSXT) were examined based on alignment results. Physicochemical properties—including amino acid length, molecular weight, theoretical isoelectric point, aliphatic index, and instability index—were predicted using ExPASy ProtParam.

To investigate evolutionary relationships, *GRF* and *GIF* protein sequences from *A. thaliana* and *O. sativa* were retrieved from TAIR. Sequences from gymnosperms, including *Picea abies*, *Ginkgo biloba*, and *Gnetum montanum*, were obtained from unpublished datasets provided by Prof. Minsheng Yang (Hebei Agricultural University) (Chen et al. 2024).

Multiple sequence alignment was performed using MUSCLE implemented in MEGA X with default parameters. Phylogenetic trees were constructed using the Maximum Likelihood (ML) method based on the Jones–Taylor–Thornton (JTT) model, with 1000 bootstrap replicates to assess branch support. Positions with gaps and missing data were treated using the partial deletion option

(95% site coverage cutoff)(Kumar et al. 2018). The resulting tree was then visualized using the iTOL online platform (http://itol.embl.de/) to provide a clear and structured representation.

2.5 Gene Structure and Conserved Motif Analysis

Exon–intron structures of *LkaGRF* and *LkaGIF* genes were extracted from the *L. kaempferi* genome annotation (GFF3 file). Gene structures were visualized using the Gene Structure View module in TBtools-II(Chen et al. 2023).

Conserved motifs were predicted using the MEME Suite. Identified motifs were annotated through comparison with Pfam and CDD databases to confirm canonical domains such as QLQ, WRC, and SSXT.

2.6 Promoter Cis-Acting Element Analysis

The 2000 bp genomic sequences upstream of the start codon of each *LkaGRF* and *LkaGIF* gene were extracted as putative promoter regions based on genome annotation data. Cis-acting regulatory elements were identified using the PlantCARE database.

2.7 RNA Isolation and RT–qPCR Analysis

Total RNA was extracted using the RNAiso Plus Plant RNA Extraction Kit (Takara, Japan). RNA integrity was assessed by 2% agarose gel electrophoresis, and concentration was measured using a Qubit fluorometer (Invitrogen).

First-strand cDNA was synthesized using the PrimeScript™ RT Reagent Kit with gDNA Eraser (Takara). Quantitative real-time PCR (RT–qPCR) was performed using a CFX96™ system (Bio-Rad) with SsoFast™ EvaGreen® Supermix. *LkaEF1A* from *L. kaempferi* was used as the internal reference gene. Relative expression levels were calculated using the $2^{-\Delta\Delta Ct}$ method. Primer sequences are provided in Table S2. Each assay included three biological replicates.

2.8 Expression Analysis of Mature miR396 During SE in *L. kaempferi*

The expression of mature miR396 was quantified across nine developmental stages of somatic embryogenesis in *L. kaempferi*. Total small RNA was isolated using the MicroRNA Kit (ZOMANBIO, Beijing, China). Reverse transcription was performed with the miRcute Enhanced miRNA cDNA Synthesis Kit (TIANGEN, Beijing, China), and the resulting cDNA was diluted 10-fold before qRT-PCR. The universal reverse primer supplied with the kit was used in combination with the miR396-specific forward primer (5′-CGGTTCCACAGCTTTCTTGAACTTA-3′). 5.8S rRNA was used as the reference gene, with the forward primer 5′-GTCTGTCTGGGCGTCGCATAA-3′. Relative expression levels were calculated using the $2^{-\Delta\Delta Ct}$ method. Three biological replicates were analyzed for each stage, and statistical significance was assessed by one-way ANOVA using SPSS 22.0 ($p < 0.05$)

2.9 5′ RLM-RACE Validation of miR396-Mediated Cleavage

Potential targeting relationships between Lka-miR396s and *LkaGRF* transcripts were predicted using the psRNATarget online tool. To validate miR396-mediated cleavage of *LkaGRF* transcripts, 5′ RNA ligase-mediated rapid amplification of cDNA ends (5′ RLM-RACE) was performed using the FirstChoice® RLM-RACE Kit (Ambion) according to the manufacturer's instructions. Briefly, 5′ RACE cDNA was synthesized from adapter-ligated mRNA. Nested PCR was then carried out using adapter-

specific primers provided in the kit together with gene-specific primers for *LkaGRF1-LkaGRF5*. The amplified products corresponding to the 5′ ends of the 3′ cleavage fragments were cloned into the pMD19-T Easy vector (TaKaRa) and sequenced. The sequencing results of the cloned products were aligned with the corresponding target gene sequences to identify miR396-guided cleavage sites and thereby verify the targeting relationships between miR396 and *LkaGRF* transcripts. In addition, the 5′ RACE cDNA was used for PCR detection of the accumulation of 3′ cleavage fragments. The gene-specific primers used for 5′ RLM-RACE are listed in Table S3.

3. Results

3.1. Genome-Wide Identification of *GRF* and *GIF* Genes

To systematically identify *GRF* and *GIF* homologs in *L. kaempferi*, bidirectional BLASTp searches were conducted using known *A. thaliana* GRF and GIF protein sequences as queries, combined with HMMER-based domain screening. The conserved QLQ and WRC domains of GRF proteins and the SSXT domain of GIF proteins were used as criteria to screen the *L. kaempferi* genome assembly. Candidate genes were amplified from cDNA derived from proembryogenic masses using PCR, followed by molecular cloning and Sanger sequencing for validation. After stringent filtering, 5 *LkaGRF* (*LkaGRF1–LkaGRF5*) and 3 *LkaGIF* (*LkaGIF1–LkaGIF3*) full-length coding sequences were confirmed.

To further characterize these family members, their physicochemical properties were analyzed and subcellular localization was predicted using bioinformatic approaches. The LkaGRFs ranged from 420 to 789 amino acids in length, with predicted molecular weights of 46.93–84.66 kDa (Table S4). Their theoretical isoelectric points (pI) ranged from 8.41 to 9.38, indicating that they are basic proteins. The LkaGRFs exhibited instability index values between 51.16 and 57.95, suggesting predicted instability. The aliphatic index ranged from 55.53 to 60.40, reflecting moderate thermostability. Grand average of hydropathicity (GRAVY) values were negative (−0.540 to −0.707), indicating hydrophilic properties.

The LkaGIFs comprise 248–272 amino acids, with predicted molecular weights of 26.61–30.13 kDa (Table S4). Their pI values ranged from 5.60 to 6.12, indicating acidic to near-neutral characteristics. Instability index values varied from 52.89 to 64.64, with LkaGIF2 showing the highest predicted instability. The aliphatic index ranged from 52.83 to 71.67, with LkaGIF3 exhibiting the highest value. All three proteins had negative GRAVY scores (−0.566 to −1.157), with LkaGIF2 predicted to be the most hydrophilic. Subcellular localization prediction suggested that all proteins are nuclear-localized, consistent with their proposed roles as transcription factors or transcriptional co-regulators

Multiple sequence alignment showed that LkaGRFs contain highly conserved QLQ (Gln-Leu-Gln) and WRC (Trp-Arg-Cys) domains at the N-terminus. The QLQ domain was strongly conserved and is thought to be important for GRF–GIF protein interactions. The WRC domain, enriched in cysteine and basic residues and containing conserved Cys and His sites, is likely involved in DNA binding and nuclear localization. LkaGIFs possess a conserved SSXT domain at the N-terminus. This domain represents the core functional region of the *GIF* family and is required for transcriptional co-

activator activity. These structural features are consistent with previously characterized *GIFs* in *A. thaliana* and *Triticum aestivum* (Figure 1B)

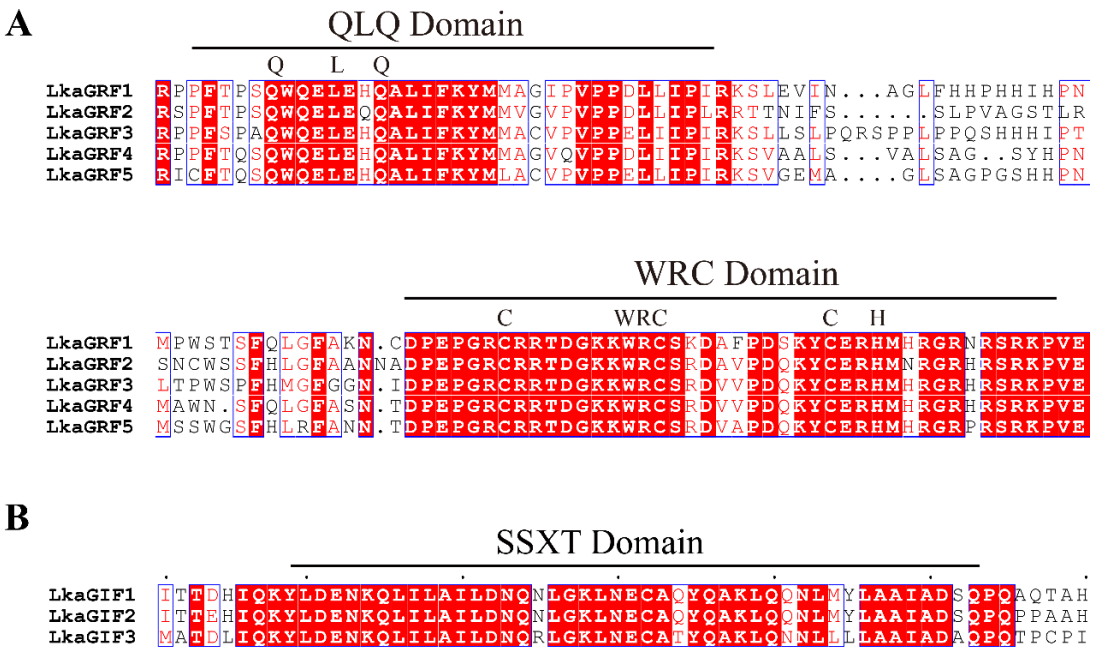

Figure 1 Multiple sequence alignment analysis of LkaGRF and LkaGIF protein sequences. (A) Alignment of the LkaGRF proteins, showing the conserved QLQ and WRC domains characteristic of the GRF family. (B) Alignment of the LkaGIF proteins, showing the conserved SSXT motif of GIF proteins. The alignment was generated using ClustalW and visualized using ESPript.

3.2. Phylogenetic and Evolutionary Analysis

To clarify the evolutionary relationships and potential functional diversification of the *GRF* and *GIF* families in *L. kaempferi*, homologous protein sequences from six representative plant species were analyzed. These included the angiosperms *A. thaliana* and *O. sativa*, and the gymnosperms *Picea abies*, *Ginkgo biloba*, *Gnetum montanum*, and *L. kaempferi*. Phylogenetic analysis of GRF revealed that sequences from the six species were divided into three major clades (Clade I–III) (Figure 2A). Each clade exhibited a clear lineage-specific distribution pattern. Clade I consisted exclusively of gymnosperm members (*P. abies*, *G. biloba*, *G. montanum*, and *L. kaempferi*). This pattern suggests that these GRFs may represent a gymnosperm-enriched lineage. Notably, four of the five *L. kaempferi* members (LkaGRF2–LkaGRF5) clustered within Clade I and formed orthologous groups with other gymnosperm GRF. In contrast, Clade III comprised only angiosperm GRF proteins from *A. thaliana* and *O. sativa*, with no gymnosperm representatives. This lineage likely expanded after the divergence of angiosperms. Clade II contained both gymnosperm and angiosperm members. Among the *L. kaempferi* genes, only LkaGRF1 was assigned to Clade II.

Phylogenetic analysis of GIF proteins further demonstrated that members from the six species were grouped into four clades (Clade I–IV) (Figure 2B). Angiosperm GIF proteins were primarily distributed in Clade I and Clade III, whereas gymnosperm members were mainly clustered in Clade II and Clade IV. LkaGIF1 and LkaGIF2 clustered with homologous gymnosperm proteins in Clade II. In contrast, LkaGIF3 grouped with *P. abies* homologs in Clade IV, forming a separate and well-supported branch.

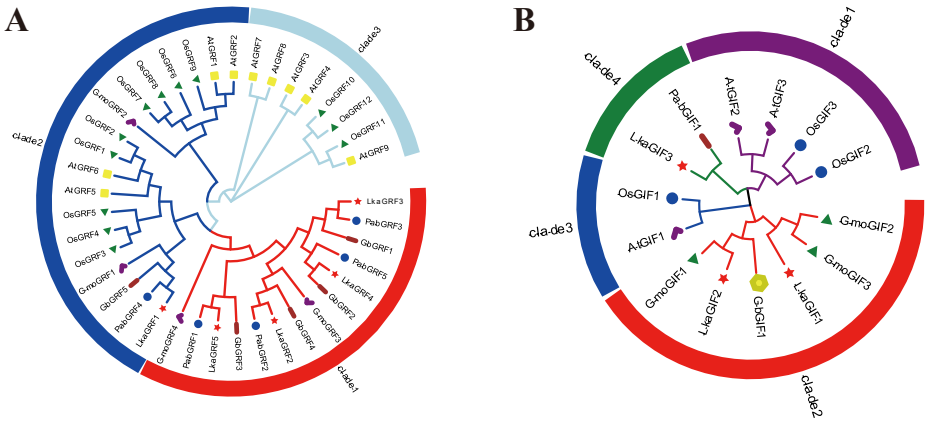

Figure 2 Phylogenetic relationships of GRF and GIF gene family members from six plant species. (A) GRF proteins were grouped into three clades (I–III).(B) GIF proteins were classified into four clades (I–IV). The trees were constructed using protein sequences from *Larix kaempferi* , *Arabidopsis thaliana*, *Oryza sativa*, *Ginkgo biloba*, *Gnetum_montanum*, and *Picea_abies.* Different colors in the outer rings represent different phylogenetic groups. Symbols with different shapes indicate proteins from different species, and the red pentagrams represent GRF and GIF proteins identified in *L.kaempferi.*

3.3. Gene Structure and Conserved Domain Analysis

To further elucidate the structural features and potential functions of the *LkaGRF* and *LkaGIF* gene families, we performed conserved motif analysis of their amino acid sequences and systematically compared their gene structures, including exon-intron organization (Figure 3A and Figure 3B).

Conserved motif analysis using MEME identified 10 conserved motifs in LkaGRF proteins. Among them, Motif 1 and Motif 2 correspond to the characteristic QLQ and WRC domains, which are mainly located in the N-terminal region of the protein. These domains are essential for the *GRF* family's core functions, including DNA binding and nuclear localization. Additionally, Motif 3 and Motif 4 correspond to the conserved FFD and TQL motifs, respectively, which are mainly located at the C-terminus and may be involved in protein stability and interactions with other proteins. Gene structure analysis revealed significant differences in gene length among *LkaGRF* family members. *LkaGRF1* lacks introns, while *LkaGRF2* contains 2 introns, *LkaGRF3* and *LkaGRF5* each contain 3 introns, and *LkaGRF4* contains 4 introns. Furthermore, with the exception of *LkaGRF4*, which

has three 3′-UTRs, all other *LkaGRF* genes contain one 5′-UTR and one 3′-UTR. The variation in exon-intron structure suggests that although all members retain conserved domains, the gene length and structure have undergone different adjustments during evolution.

Conserved motif analysis of the *LkaGIF* family identified 10 conserved motifs through MEME. *LkaGIF1* contains 10 motifs, *LkaGIF2* contains 8 motifs, and *LkaGIF3* contains only 5 motifs. Among these motifs, Motif 1 is the characteristic SSXT superfamily domain, which is completely retained in all *LkaGIF* members and shows a high degree of conservation. This suggests that this domain may be closely related to the functional specificity of the GIF protein family.

Gene structure analysis revealed that all *LkaGIF* genes contain both 5′-UTR and 3′-UTR, and each gene has 3 introns. Minor differences in the position and length of introns were observed among the *LkaGIF* family members, indicating that although the GIF family maintains a relatively conserved structure, there is still some degree of structural diversity.

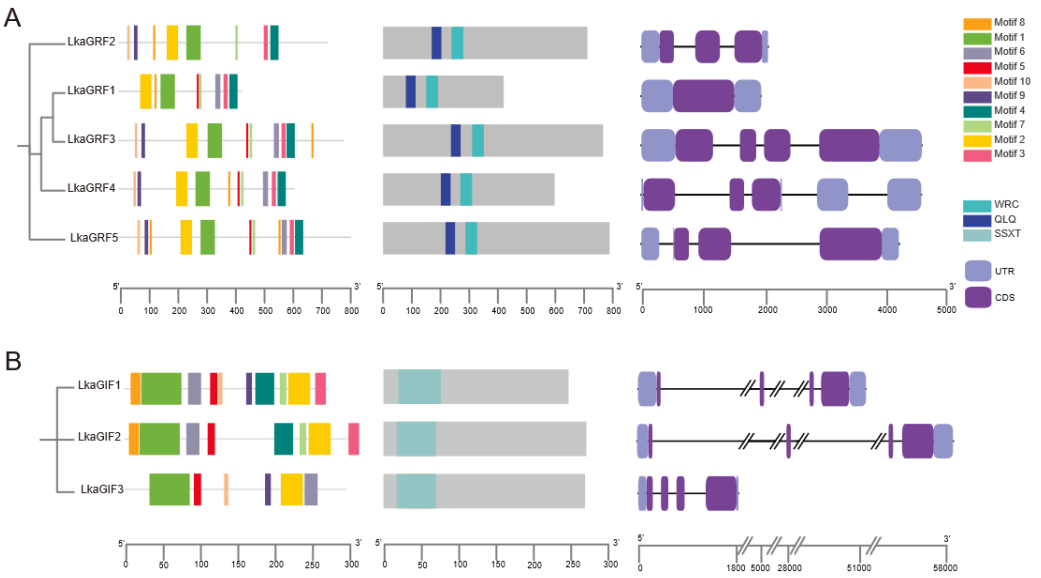

Figure 3 Structural organization and conserved motif composition of *LkaGRF* and *LkaGIF* gene families. (A) Analysis of the *LkaGRF* gene family. (B) Analysis of the *LkaGIF* gene family. From left to right, the panels show the phylogenetic relationships, conserved motif composition, conserved domains, and gene structures of each gene. Different colored boxes represent different conserved motifs. The QLQ and WRC domains are indicated in LkaGRF proteins, whereas the SSXT domain is shown in LkaGIF proteins. In the gene structure panel, lines represent introns, light purple boxes indicate untranslated regions (UTRs), and dark purple boxes indicate coding sequences (CDSs).

3.4. Cis-Acting Elements in Promoter Regions

To further explore the potential regulatory mechanisms of *LkaGRF* and *LkaGIF* genes at the transcriptional level, a detailed cis-regulatory element analysis of their promoter regions was performed (Figure 4). The results revealed that the promoter regions of both *LkaGRF* and *LkaGIF* genes are enriched with cis-elements related to growth and development, light response, phytohormone response, and stress-related responses. In the phytohormone response analysis, multiple phytohormone-responsive elements were identified in the promoters of both *LkaGRF* and *LkaGIF* genes, suggesting their potential involvement in phytohormone signaling pathways.

Specifically, phytohormone-responsive elements such as ABRE (ABA response), CGTCA-motif/TGACG-motif (JA response), ERE (ETH response), AuxRE (IAA response), P-box/GARE-motif (GA response), and TCA-element/SARE (SA response) were detected. The presence of these elements suggests that LkaGRF and LkaGIF genes may be transcriptionally responsive to multiple phytohormone-related signals. Notably, *LkaGRF3* contained 5 ABRE elements, and *LkaGRF5* contained 3 ERE elements. In the *LkaGIF* family, the promoters of all three genes (LkaGIF1-3) contained ABRE elements, and *LkaGIF3* also contained an AuxRE element, suggesting that LkaGIF3 might be involved in IAA-induced responses. In conclusion, both *LkaGRF* and *LkaGIF* gene families are enriched with phytohormone-responsive cis-elements in their promoters, indicating that these genes may jointly participate in the regulation of multiple phytohormone signaling pathways and play important roles in plant growth, development, and stress responses.

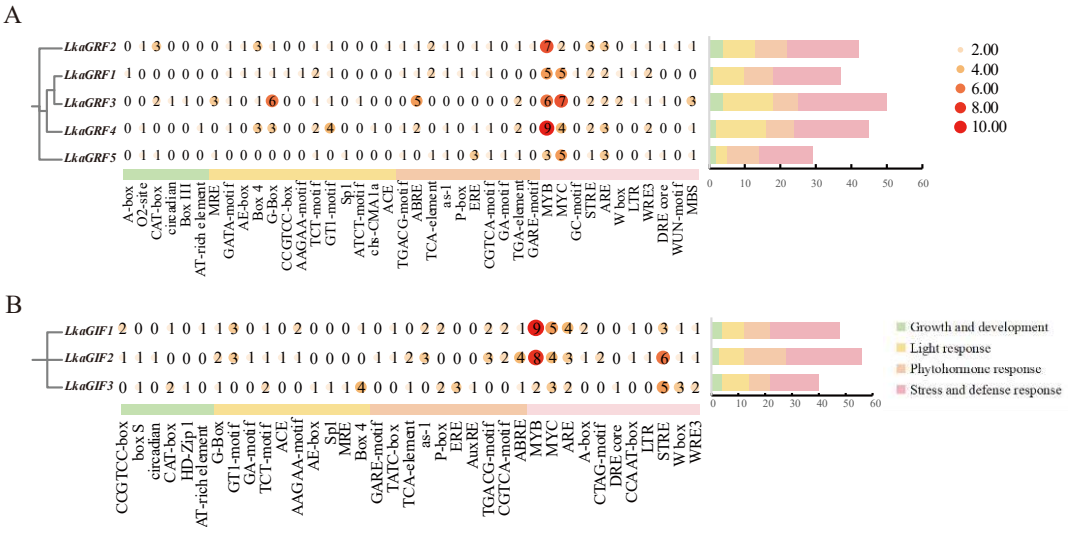

Figure 4 Analysis of cis-acting regulatory elements in the promoter regions of *LkaGRF* and *LkaGIF* genes. A) Distribution of predicted cis-acting elements in the promoter regions of *LkaGRF* family members. B) Distribution of predicted cis-acting elements in the promoter regions of *LkaGIF* family members. The colored bars represent different types of cis-regulatory elements: green for growth and development, yellow for light response, pink for phytohormone response, and red for stress and defense response. The size of each circle represents the relative abundance of each cis-element.

3.5. Prediction of miR396 Target Sites in *LkaGRF* Transcripts

Target interactions between *Lka-miR396* family members (*Lka-miR396a*, *Lka-miR396b*, and *Lka-miR396c*) and *LkaGRF* transcripts were predicted using psRNATarget. The analysis showed that miR396 members exhibit strong sequence complementarity with *LkaGRF1–LkaGRF5* transcripts. The predicted cleavage sites were located within the coding regions of each *LkaGRF* gene, and the targeting patterns were highly conserved (Figure 5). Sequence alignment indicated that *Lka-miR396a*, *Lka-miR396b*, and *Lka-miR396c* display perfect or near-perfect base pairing with their respective target sequences in *LkaGRF* genes, with only minor mismatches or small gaps at a few nucleotide positions. Although the target site of *LkaGRF5* contains a single nucleotide variation at the 5′ end, the overall complementarity pattern remains largely unchanged, suggesting that miR396-mediated targeting may be conserved across the *LkaGRF* family.

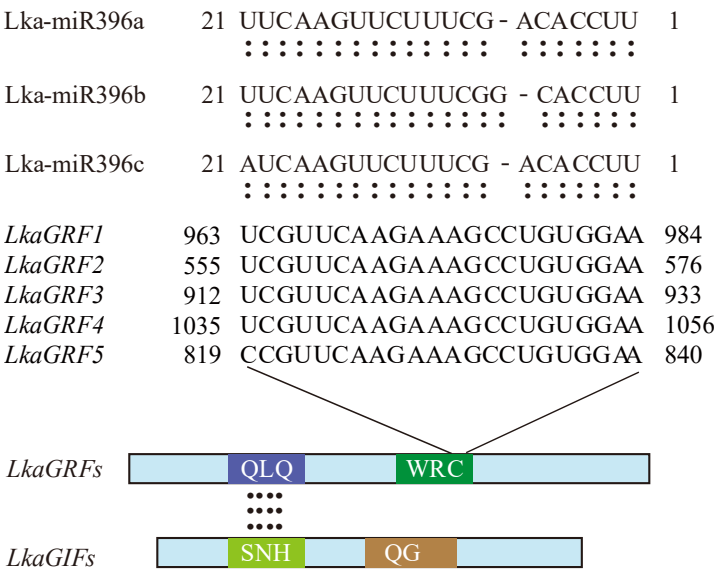

Figure 5 Prediction analysis of the targeting relationships between Lka-miR396 family members and *LkaGRF* transcripts. The upper panel shows the complementary pairing between Lka-miR396 and *LkaGRF* transcripts, where dashed lines indicate nucleotide pairing. The lower panel illustrates the conserved domains of LkaGRF and LkaGIF proteins.

To verify whether Lka-miR396a cleaves its predicted *LkaGRF* targets, 5'RLM-RACE was performed on *LkaGRF* transcripts. Clear and specific amplification bands were detected only for *LkaGRF3* and *LkaGRF5* (Figure 6A). Cloning and sequencing of the RLM-RACE products further confirmed distinct miRNA-mediated cleavage sites in both genes (Figure 6B). In *LkaGRF3*, all 10 independent clones had 5′ ends corresponding to the 11th nucleotide from the 5′ end of Lka-miR396a. In *LkaGRF5*, 9 out of 10 clones showed cleavage at the same position. Together, these results support that Lka-miR396a specifically cleaves *LkaGRF3* and *LkaGRF5* at the predicted target sites. The absence of detectable 5′ RLM-RACE products for the other *LkaGRFs* may reflect low cleavage abundance, tissue-specific cleavage activity, low transcript abundance, or technical limitations of the assay, rather than definitive absence of miR396-mediated regulation.

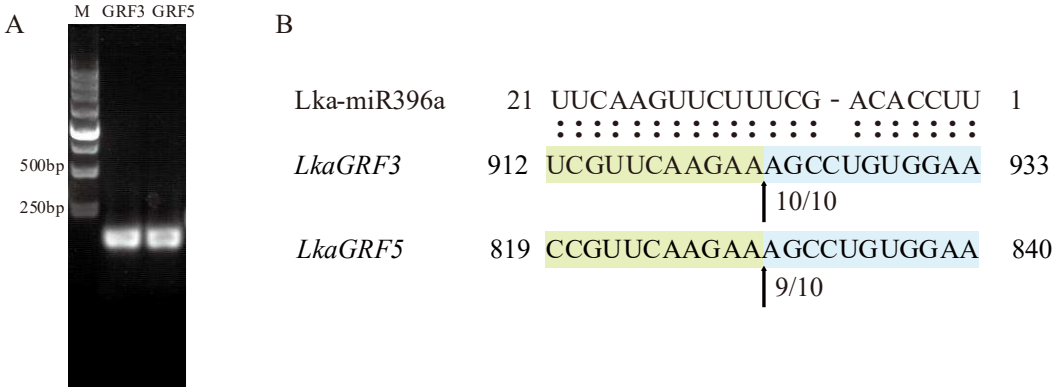

Figure 6 5'RLM-RACE validation of *LkaGRF* cleavage mediated by Lka-miR396a. (A) 5'RLM-RACE analysis was conducted for *LkaGRF1–LkaGRF5* transcripts, and clear, specific amplification products were detected only for *LkaGRF3* and *LkaGRF5*; M indicates the 250 bp DNA marker. (B) Complementary pairing between Lka-miR396a and the *LkaGRF3* and *LkaGRF5* transcripts, showing the miRNA-mediated cleavage sites. Arrows indicate the cleavage positions, and numbers represent the proportion of sequenced clones supporting each cleavage site.

3.6. Expression Pattern Analysis During Somatic Embryogenesis

To investigate the potential roles of *LkaGRFs*, *LkaGIFs*, and Lka-miR396a during somatic embryogenesis in *Larix kaempferi*, their transcript levels were quantified at different developmental stages. Both gene families exhibited dynamic and stage-dependent expression patterns (Figure 7). Although transcript levels fluctuated between days 2 and 21, no statistically significant differences were detected among these early stages. According to our previous developmental stage classification of somatic embryogenesis in *L. kaempferi*, somatic embryos enter the early cotyledonary stage at 21–28 days after induction. Consistent with this staging, the transcript levels of most *LkaGRF* and *LkaGIF* genes increased significantly from day 21 to day 28 and reached their highest levels at day 28. Subsequently, somatic embryos entered the middle cotyledonary stage during 28–35 days and developed into mature embryos during 35–42 days, during which the expression levels of most *LkaGRF* and *LkaGIF* genes gradually declined. Lka-miR396a displayed a distinct temporal expression pattern. Its transcript level increased significantly from 0 to 2 days, followed by a decrease between 2 and 10 days. Thereafter, expression levels gradually increased again and reached the highest level at day 28. These results suggest that *LkaGRF*, *LkaGIF*, and Lka-miR396a exhibit coordinated yet distinct expression dynamics during somatic embryogenesis and may be associated with cotyledonary embryo growth and development in *L. kaempferi*.

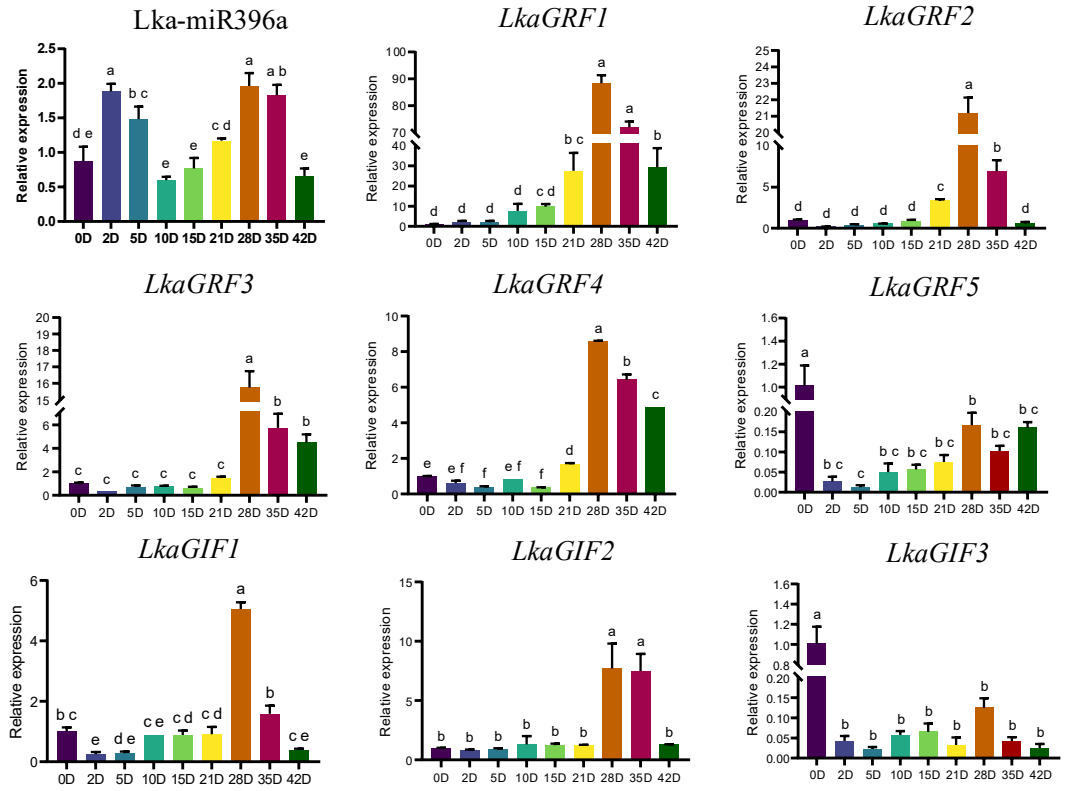

Figure 7 Expression profiles of *LkaGRF* and *LkaGIF* genes during somatic embryogenesis. Relative expression levels of *LkaGRF1–5* and *LkaGIF1–3* were analyzed by qRT-PCR at different developmental stages (0, 2, 5, 10, 15, 21, 28, 35, and 42 days after induction). Data are means ± standard error (SE) of three independent biological replicates. Different lowercase letters above the bars indicate

statistically significant differences among stages ($P < 0.05$, Duncan's multiple range test). The relative expression was normalized to the reference gene *LkaEF1A* with the 0-day sample set as 1.

3.7. Expression patterns of *LkaGRF* and *LkaGIF* genes in embryogenic cell lines of *L. kaempferi* under different phytohormone treatments

qRT-PCR analysis revealed that the five *LkaGRF* genes exhibited distinct transcriptional responses to exogenous hormone treatments (Figure 8). Overall, most *LkaGRF* genes were downregulated to varying degrees following IAA, ABA, GA, JA, and SA treatments, although the magnitude and timing of the responses differed substantially among family members. *LkaGRF1* showed a generally suppressed expression pattern under all five hormone treatments, with only slight recovery at later time points under GA, JA, and SA. Similarly, *LkaGRF3* and *LkaGRF5* were markedly repressed by IAA, ABA, GA and SA, indicating that these genes are highly sensitive to multiple hormone signals. In contrast, *LkaGRF2* and *LkaGRF4* displayed more dynamic and time-dependent expression profiles. *LkaGRF2* was initially inhibited by IAA, but its transcript abundance partially recovered at later stages; under ABA treatment, its expression fluctuated markedly and increased again at 12h and 48h. By contrast, JA maintained *LkaGRF2* expression at a consistently low level. Among all genes examined, *LkaGRF4* exhibited the strongest hormonal responsiveness. Its expression gradually increased after an initial decline under IAA treatment, reaching a relatively high level at 48h, while JA strongly induced its expression, with a prominent peak at 24h. Notably, the responses of *LkaGRF* genes to JA were highly divergent, suggesting potential functional differentiation of these family members in jasmonate signaling. Taken together, these results indicate that *LkaGRF* genes are differentially responsive to multiple phytohormone treatments in embryogenic tissues of *L. kaempferi*.

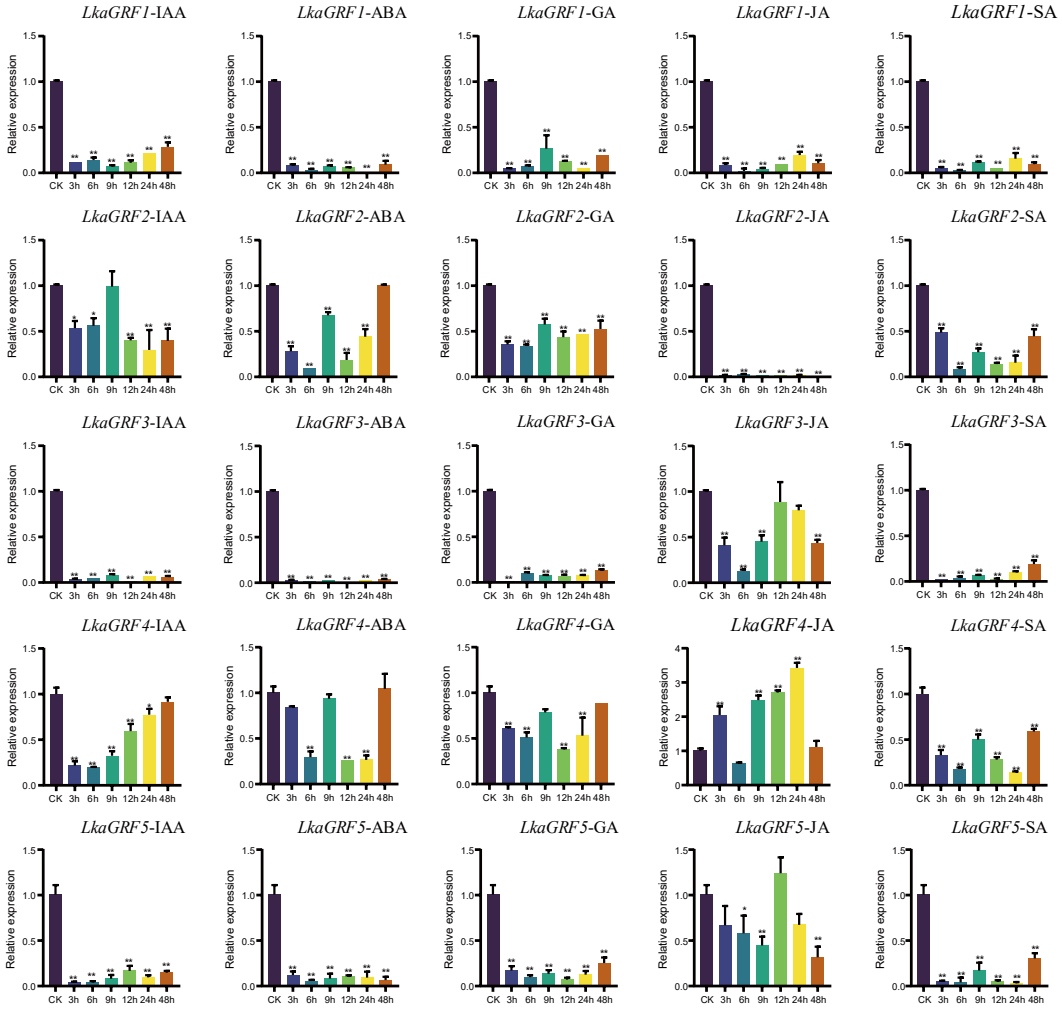

Figure 8 Expression analysis of *LkaGRFs* under IAA, ABA, GA, JA, and SA treatments. Expression profiles of five *LkaGRF* genes in embryogenic cell lines of *L. kaempferi* under different phytohormone treatments. Embryogenic cells were treated with 50 μM SA, 50 μM GA, 50 μM ABA, 50 μM IAA, and 50 μM JA, and samples were collected at 0, 3, 6, 9, 12, 24, and 48 h after treatment. Gene expression levels were determined by qRT-PCR. Error bars represent the standard deviation of three biological replicates. Asterisks indicate significant differences compared with the control ($P < 0.05$, $P < 0.01$).

All three *LkaGIF* genes exhibited clear, hormone-specific temporal responses (Figure 9). Under IAA, ABA, and SA treatments, *LkaGIF1* and *LkaGIF2* were significantly downregulated at early stages (3–9h) and then markedly upregulated at 24–48h, with the highest levels observed at 48 h. A similar downregulation–upregulation pattern was observed for *LkaGIF3* under the same three hormones.In response to GA, *LkaGIF3* showed the strongest induction, with transcript levels increasing significantly from 12 h onward and peaking at 24 h. *LkaGIF1* and *LkaGIF2* displayed moderate upregulation only at later stages (24–48h). Under JA treatment, *LkaGIF3* was dramatically induced, reaching its maximum expression at 24 h ($P < 0.01$), which represented the strongest response among all hormone–gene combinations tested. In contrast, *LkaGIF1* and *LkaGIF2* remained at low expression levels throughout the 48h period under JA.

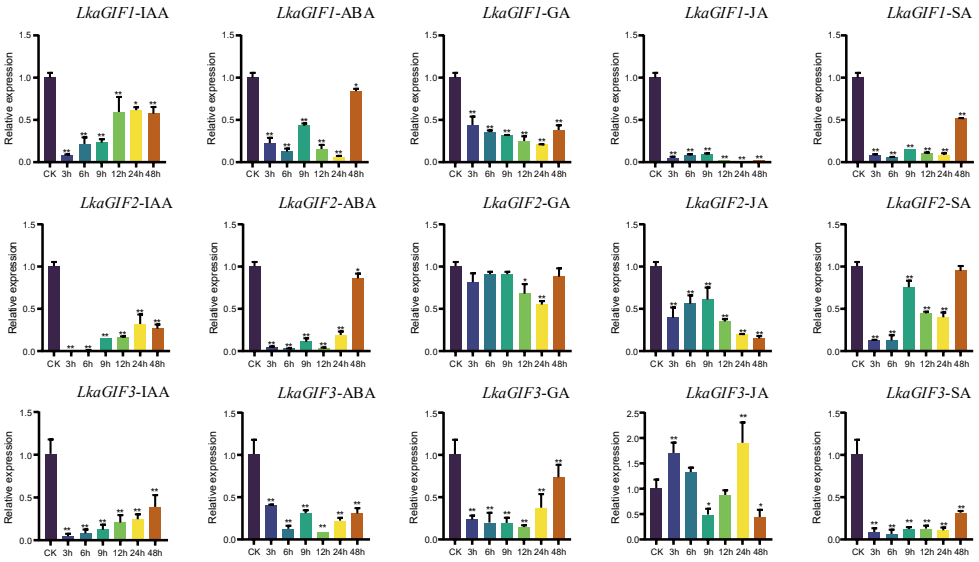

Figure 9 Expression analysis of *LkaGIFs* under IAA, ABA, GA, JA, and SA treatments. Expression profiles of three *LkaGIF* genes in embryogenic cell lines of *L. kaempferi* under different phytohormone treatments. Embryogenic cells were treated with 50 μM SA, 50 μM GA, 50 μM ABA, 50 μM IAA, and 50 μM JA, and samples were collected at 0, 3, 6, 9, 12, 24, and 48 h after treatment. Gene expression levels were determined by qRT-PCR. Error bars represent the standard deviation of three biological replicates. Asterisks indicate significant differences compared with the control ($P < 0.05$, $P < 0.01$).

4. Discussion

This study characterized the *GRF* and *GIF* gene families in *L. kaempferi* based on a well-defined somatic embryogenesis (SE) system. Through the integration of gene family identification, phylogenetic analysis, miRNA target prediction and validation, developmental expression profiling, and hormone-response analysis, *LkaGRF* and *LkaGIF* genes were identified as candidate regulators associated with SE-related developmental transitions. When combined with morphological characterization of embryogenic stages, these findings further suggest that the miR396–GRF/GIF regulatory axis may be associated with cotyledonary embryo development and hormone-responsive developmental regulation in this conifer species.

4.1 Identification, Evolution, and Characterization of the GRF and GIF Gene Families

In this study, five *GRF* genes and three *GIF* genes were identified and cloned from *L. kaempferi*. All LkaGRF proteins retained the typical QLQ and WRC domains(Kim et al. 2003; Choi et al. 2004). These structural features were highly consistent with those reported for GRF proteins in model plants such as *Arabidopsis thaliana* and *Oryza sativa*. The QLQ domain mediates interaction with GIF proteins, whereas the WRC domain is responsible for DNA binding and nuclear localization(Liebsch and Palatnik 2020). All LkaGRF proteins were predicted to localize to the nucleus, supporting their molecular role as transcriptional regulators. This finding is consistent with previous reports in *A. thaliana*, *O. sativa*, and *M. dodecandrum*(Choi et al. 2004; Kim 2019; Huang et al. 2023).

Phylogenetic analysis showed that *LkaGRF2-LkaGRF5* and *LkaGIF1-LkaGIF2* clustered with gymnosperm-associated branches, indicating that the *GRF* and *GIF* families are broadly conserved across seed plants while also showing lineage-associated diversification in gymnosperms. Although phylogenetic clustering alone does not imply functional divergence, these patterns provide a useful framework for identifying candidate regulators involved in conifer somatic embryogenesis.

4.2 Conservation of the miR396–GRF Module and Its Role in Somatic Embryogenesis

Somatic embryogenesis (SE) is a dynamic reprogramming process involving the acquisition of embryogenic competence, sustained cell proliferation, embryo differentiation, and subsequent maturation(Ikeuchi et al. 2013; Fehér 2019). Increasing evidence suggests that this process is regulated not only by transcription factors, but also by the coordinated action of small RNAs and phytohormone signaling pathways(Wójcikowska et al. 2013, 2024; Zhu et al. 2022; Pierroz 2023). Among these regulators, the miR396–GRF–GIF module appears to play an important role in controlling embryogenic development.

In *Arabidopsis*, miR396 accumulates in embryogenesis-inducing regions and is closely associated with sensitivity to exogenous 2,4-D. It regulates SE induction by targeting several *GRF* genes and affecting auxin-related and *PLT* associated pathways, indicating a direct role in the early establishment of embryogenic competence (Wójcikowska et al. 2018). Similar observations have also been reported in other species. In lily and hybrid *Liriodendron*, miR396 and its candidate *GRF* targets were identified as components of SE-associated regulatory networks, suggesting that this module may participate in embryo development across multiple plant species (Li et al. 2012; Zhang et al. 2017).

More direct functional evidence has been obtained in regeneration systems. In *Hevea brasiliensis*, *HbGRF4* and *HbGIF1* were significantly upregulated during SE, and overexpression of *HbGRF4* or *HbGRF4–HbGIF1* increased embryogenesis efficiency (Luo et al. 2024). In soybean, the *GRF3–GIF1* chimera markedly improved regeneration and transformation efficiency, and this effect was further enhanced when the miR396 target site was mutated to generate an miR396-resistant form(Debernardi et al. 2020). Similar promotive effects of GRF–GIF chimeras have also been reported in wheat and tomato (Kim 2019; Lu et al. 2022; Yarra and Krysan 2023). Together, these studies suggest that the miR396–GRF–GIF pathway is closely associated with somatic embryogenesis and regeneration-related processes in several plant species.

Importantly, our previous work provides additional phenotypic support for the developmental significance of this regulatory pathway in *L. kaempferi*. Somatic embryos overexpressing miR396 exhibited irregular cotyledon outlines, abnormal variation in cotyledon cell size, and disorganized root apical structures. In addition, these transgenic lines showed reduced germination and rooting rates, together with a significantly increased frequency of abnormal leaf number. When considered together with the present results, including target site prediction and validation, developmental expression profiling, and hormone-responsive expression patterns, these findings support a close association between the miR396–GRF/GIF regulatory axis and somatic embryogenesis in *L.*

kaempferi. In particular, this module appears to be associated with cotyledon formation, embryo morphological patterning, and subsequent germination and rooting performance. Therefore, the miR396–GRF/GIF pathway may represent an important regulatory component influencing cotyledonary embryo development and embryo quality in the larch SE system.

4.3 Hormone Responsiveness of *LkaGRF* and *LkaGIF* Genes

Somatic embryogenesis is a hormone-dependent developmental reprogramming process in which multiple phytohormone signaling pathways interact to regulate embryogenic competence, cell fate transitions, embryo differentiation, and subsequent developmental progression (Fehér 2015; Kaizhuan et al. 2018; Chen et al. 2021). In the present study, promoter analysis identified abundant hormone-responsive cis-elements, including ABRE, AuxRE, CGTCA-motif, and ERE, in the promoter regions of *LkaGRF* and *LkaGIF* genes, suggesting that these genes may be transcriptionally responsive to diverse hormonal signals.

Consistent with this prediction, RT-qPCR analysis showed that both *LkaGRF* and *LkaGIF* genes responded rapidly and differentially to exogenous hormone treatments. Most *LkaGRF* genes were downregulated to varying degrees after IAA, ABA, GA, and SA treatments, particularly at early time points (3-6 h), indicating a rapid transcriptional response to hormonal perturbation. In contrast, *LkaGRF4* displayed a distinct expression pattern and was strongly induced under JA treatment. Similarly, among the three *LkaGIF* genes, *LkaGIF3* showed pronounced induction in response to JA, whereas the other members exhibited relatively moderate or delayed responses. These results indicate that different members of the *LkaGRF* and *LkaGIF* families differ in their responsiveness to hormonal cues and may therefore participate in different aspects of hormone-associated developmental regulation.

Interactions between GRF and hormone signaling pathways have been reported in several plant species. In *O. sativa*, the OsmiR396–OsGRF module regulates GA signaling through DELLA proteins and IDD2, while brassinosteroid signaling modulates miR396 expression via BZR1 to control OsGRF4 mediated plant architecture and leaf angle(Choi et al. 2004; Li et al. 2016; Tang et al. 2018). In addition, under cold stress conditions, GRF has been shown to interact with DELLA proteins to regulate growth inhibition(Shahan 2020), further highlighting the close association between *GRF* activity and hormone-related developmental control. Although comparable regulatory relationships have not yet been functionally demonstrated in *L. kaempferi*, the hormone-responsive expression patterns observed here suggest that *LkaGRF* and *LkaGIF* genes may also be integrated into hormone-associated transcriptional networks.

In combination with the stage-specific expression patterns of *LkaGRF* and *LkaGIF* genes during cotyledonary embryo development, these findings support the view that the miR396-GRF/GIF regulatory axis is closely associated with key developmental events in the larch SE system, including cotyledon formation, embryo morphogenesis, and the establishment of normal developmental competence(Xiao et al. 2016). Therefore, rather than acting as direct regulators of individual hormone pathways, *LkaGRF* and *LkaGIF* genes are more likely to function as

components of a broader hormone-responsive regulatory framework affecting cotyledonary embryo development and embryo quality in *L. kaempferi*.

5. Conclusions

This study identified and characterized *LkaGRF* and *LkaGIF* genes in *L. kaempferi* and demonstrated that the miR396–GRF/GIF module is conserved and dynamically regulated during somatic embryogenesis. Peak expression during the cotyledonary transition and differential hormone responsiveness suggest that this module is associated with cotyledonary embryo development and embryo quality. These findings provide candidate regulators for future functional studies in conifer somatic embryogenesis.

Declarations

Supplementary Materials:

Author Contributions: Writing: original draft preparation, Y.H.; methodology, X.L.; supervision, R.Z.; supervision, L.Q.; writing: review and editing, supervision, L.Z.; All authors have read and agreed to the published version of the manuscript.

Funding: This project was funded by the National Natural Science Foundation of China (32171811), the National Key R&D Program of China (2022YFD2200302), and the Biological Breeding-National Science and Technology Major Project (2023ZD0405802).

Data Availability Statement: All data in this study can be found in the manuscript or the Supplementary Materials.

Acknowledgments: The authors acknowledge the programs that provided financial support for this study.

Conflicts of Interest: The authors have no relevant financial or non-financial interests to disclose.

References

Alongi F, Petek-Petrik A, Mukarram M, et al (2025) Somatic drought stress memory affects leaf morpho-physiological traits of plants via epigenetic mechanisms and phytohormonal signalling. Plant Gene 42:100509. https://doi.org/10.1016/j.plgene.2025.100509

Bull T, Debernardi J, Reeves M, et al (2023) GRF–GIF chimeric proteins enhance *in vitro* regeneration and Agrobacterium-mediated transformation efficiencies of lettuce (*Lactuca* spp.). Plant Cell Rep 42:629–643. https://doi.org/10.1007/s00299-023-02980-4

Chen B, Fiers M, Dekkers BJW, et al (2021) ABA signalling promotes cell totipotency in the shoot apex of germinating embryos. Journal of Experimental Botany 72:6418–6436. https://doi.org/10.1093/jxb/erab306

Chen C, Wu Y, Li J, et al (2023) TBtools-II: A "one for all, all for one" bioinformatics platform for biological big-data mining. Molecular Plant 16:1733–1742. https://doi.org/10.1016/j.molp.2023.09.010

Chen X, Zhang J, Wang S, et al (2024) Genome-wide molecular evolution analysis of the *GRF* and *GIF* gene families in Plantae (Archaeplastida). BMC Genomics 25:74. https://doi.org/10.1186/s12864-024-10006-w

Choi D, Kim JH, Kende H (2004) Whole genome analysis of the *OsGRF* gene family encoding plant-specific putative transcription activators in rice (*Oryza sativa* L.). Plant and Cell Physiology 45:897–904. https://doi.org/10.1093/pcp/pch098

Debernardi JM, Tricoli DM, Ercoli MF, et al (2020) A *GRF–GIF* chimeric protein improves the regeneration efficiency of transgenic plants. Nature Biotechnology 38:1274–1279. https://doi.org/10.1038/s41587-020-0703-0

Duan H, Maren NA, Ranney TG, Liu W (2022) New opportunities for using *WUS*/*BBM* and *GRF*-*GIF* genes to enhance genetic transformation of ornamental plants. Ornamental Plant Research 2:1–7. https://doi.org/10.48130/OPR-2022-0004

Fan Y, Li W, Li Z, et al (2021) Examination of the transcriptional response to *LaMIR166a* overexpression in *Larix kaempferi* (Lamb.) Carr. Biology 10:576. https://doi.org/10.3390/biology10070576

Fan Y, Li Z, Zhang L, et al (2020) Metabolome and transcriptome association analysis reveals regulation of flavonoid biosynthesis by overexpression of *LaMIR166a* in *Larix kaempferi* (Lamb.) Carr. Forests 11:1367. https://doi.org/10.3390/f11121367

Fehér A (2019) Callus, dedifferentiation, totipotency, somatic embryogenesis: what these terms mean in the era of molecular plant biology? Frontiers in Plant Science 10:536. https://doi.org/10.3389/fpls.2019.00536

Fehér A (2015) Somatic embryogenesis—stress-induced remodeling of plant cell fate. Biochimica et Biophysica Acta (BBA) - Gene Regulatory Mechanisms 1849:385–402. https://doi.org/10.1016/j.bbagrm.2014.07.005

Filonova LH, Bozhkov PV, Arnold SV (2000) Developmental pathway of somatic embryogenesis in *Picea abies* as revealed by time-lapse tracking. Journal of Experimental Botany 51:249–264. https://doi.org/10.1093/jexbot/51.343.249

Fu M-K, He Y-N, Yang X-Y, et al (2024) Genome-wide identification of the *GRF* family in sweet orange (*Citrus sinensis*) and functional analysis of the *CsGRF04* in response to multiple abiotic stresses. BMC Genomics 25:37. https://doi.org/10.1186/s12864-023-09952-8

Huang J, Chen G-Z, Ahmad S, et al (2023) Genome-wide identification and characterization of the *GRF* gene family in *Melastoma dodecandrum*. International Journal of Molecular Sciences 24:1261. https://doi.org/10.3390/ijms24021261

Ikeuchi M, Sugimoto K, Iwase A (2013) Plant callus: mechanisms of induction and repression. Plant Cell 25:3159–3173. https://doi.org/10.1105/tpc.113.116053

Inger H, Larry CF, Sara Von A, Tage E (1985) The development of somatic embryos in tissue cultures initiated from immature embryos of *Picea abies* (Norway spruce). Plant Science 38:53–59. https://doi.org/10.1016/0168-9452(85)90079-2

Iqbal S, Wang X, Mubeen I, et al (2022) Phytohormones trigger drought tolerance in crop plants: outlook and future perspectives. Frontiers in Plant Science 12:799318. https://doi.org/10.3389/fpls.2021.799318

Kaizhuan X, Xiaohui M, Yingheng W, et al (2018) Transcript profiling reveals abscisic acid, salicylic acid and jasmonic-isoleucine pathways involved in high regenerative capacities of immature embryos compared with mature seeds in rice. Rice Science 25:227–234. https://doi.org/10.1016/j.rsci.2018.06.006

Kang Y, Li W, Zhang L, Qi L (2021) Over-expression of the cell-cycle gene *LaCDKB1;2* promotes cell proliferation and the formation of normal cotyledonary embryos during *Larix kaempferi* somatic embryogenesis. Genes 12:1435. https://doi.org/10.3390/genes12091435

Kim JH (2019) Biological roles and an evolutionary sketch of the *GRF-GIF* transcriptional complex in plants. BMB Reports 52:227–238. https://doi.org/10.5483/BMBRep.2019.52.4.051

Kim JH, Choi D, Kende H (2003) The *AtGRF* family of putative transcription factors is involved in leaf and cotyledon growth in *Arabidopsis*. The Plant Journal 36:94–104. https://doi.org/10.1046/j.1365-313X.2003.01862.x

Kumar S, Stecher G, Li M, et al (2018) MEGA X: molecular evolutionary genetics analysis across computing platforms. Molecular Biology and Evolution 35:1547–1549. https://doi.org/10.1093/molbev/msy096

Lee G-H, Lee BH, Jung J-H, et al (2022) Systematic assessment of the positive role of *Arabidopsis thaliana* GROWTH-REGULATING FACTORs in regulation of cell proliferation during leaf growth. Journal of Plant Biology 65:413–422. https://doi.org/10.1007/s12374-022-09366-1

Li S, Gao F, Xie K, et al (2016) The *OsmiR396c–OsGRF4–OsGIF1* regulatory module determines grain size and yield in rice. Plant Biotechnology Journal 14:2134–2146. https://doi.org/10.1111/pbi.12569

Li T, Chen J, Qiu S, et al (2012) Deep sequencing and microarray hybridization identify conserved and species-specific microRNAs during somatic embryogenesis in hybrid yellow poplar. PLoS ONE 7:e43451. https://doi.org/10.1371/journal.pone.0043451

Liebsch D, Palatnik JF (2020) MicroRNA *miR396*, *GRF* transcription factors and *GIF* co-regulators: a conserved plant growth regulatory module with potential for breeding and biotechnology. Current Opinion in Plant Biology 53:31–42. https://doi.org/10.1016/j.pbi.2019.09.008

Lu Y, Zeng J, Liu Q (2022) The rice *miR396-GRF-GIF-SWI/SNF* module: a player in GA signaling. Frontiers in Plant Science 12:786641. https://doi.org/10.3389/fpls.2021.786641

Luo G, Palmgren M (2021) *GRF-GIF* chimeras boost plant regeneration. Trends in Plant Science 26:201–204. https://doi.org/10.1016/j.tplants.2020.12.001

Luo X, Zhang Y, Zhou M, et al (2024) Overexpression of *HbGRF4* or *HbGRF4-HbGIF1* chimera improves the efficiency of somatic embryogenesis in *Hevea brasiliensis*. International Journal of Molecular Sciences 25:2921. https://doi.org/10.3390/ijms25052921

Nagmani R, Bonga JM (1985) Embryogenesis in subcultured callus of *Larix decidua*. Canadian Journal of Forest Research 15:1088–1091. https://doi.org/10.1139/x85-177

Pierroz G (2023) Making babies: how auxin regulates somatic embryogenesis in *Arabidopsis* tissue culture. The Plant Journal 113:5–6. https://doi.org/10.1111/tpj.16062

Qu L, Wang Y, Masyagina O, et al (2022) Larch: a promising deciduous conifer as an eco-environmental resource. In: Cristina Gonçalves A, Fonseca T (eds) Conifers - Recent Advances. IntechOpen

Shahan R (2020) The cold never bothered me anyway: DELLA-interacting growth regulating factors mediate plant growth in cold stress. Plant Cell 32:797–798. https://doi.org/10.1105/tpc.20.00079

Shmakov VN, Konstantinov YuM (2020) Somatic embryogenesis in *Larix*: the state of art and perspectives. Vestn VOGiS 24:575–588. https://doi.org/10.18699/VJ20.651

Szczygieł-Sommer A, Gaj MD (2019) The *miR396–GRF* regulatory module controls the embryogenic response in *Arabidopsis* via an auxin-related pathway. International Journal of Molecular Sciences 20:5221. https://doi.org/10.3390/ijms20205221

Tang Y, Liu H, Guo S, et al (2018) *OsmiR396d* affects gibberellin and brassinosteroid signaling to regulate plant architecture in rice. Plant Physiology 176:946–959. https://doi.org/10.1104/pp.17.00964

Wang J, Song L, Gong X, et al (2020) Functions of jasmonic acid in plant regulation and response to abiotic stress. International Journal of Molecular Sciences 21:1446. https://doi.org/10.3390/ijms21041446

Wójcikowska B, Botor M, Morończyk J, et al (2018) Trichostatin A triggers an embryogenic transition in *Arabidopsis* explants via an auxin-related pathway. Frontiers in Plant Science 9:1353. https://doi.org/10.3389/fpls.2018.01353

Wójcikowska B, Chwiałkowska K, Nowak K, et al (2024) Transcriptomic profiling reveals histone acetylation-regulated genes involved in somatic embryogenesis in *Arabidopsis thaliana*. BMC Genomics 25:788. https://doi.org/10.1186/s12864-024-10623-5

Wójcikowska B, Jaskóła K, Gąsiorek P, et al (2013) *LEAFY COTYLEDON2 (LEC2)* promotes embryogenic induction in somatic tissues of *Arabidopsis*, via *YUCCA*-mediated auxin biosynthesis. Planta 238:425–440. https://doi.org/10.1007/s00425-013-1892-2

Xu J, Zhang G, Zhao Z, et al (2021) Effects of randomized management on the forest distribution patterns of *Larix kaempferi* plantation in Xiaolongshan, Gansu Province, China. Forests 12:981. https://doi.org/10.3390/f12080981

Yarra R, Krysan PJ (2023) *GRF-GIF* duo and *GRF-GIF-BBM*: novel transformation methodologies for enhancing regeneration efficiency of genome-edited recalcitrant crops. Planta 257:60. https://doi.org/10.1007/s00425-023-04096-1

Yu Y, Sun F, Chen N, et al (2021) *MiR396* regulatory network and its expression during grain development in wheat. Protoplasma 258:103–113. https://doi.org/10.1007/s00709-020-01556-3

Zhang J, Xue B, Gai M, et al (2017) Small RNA and transcriptome sequencing reveal a potential miRNA-mediated interaction network that functions during somatic embryogenesis in *Lilium pumilum* DC. Fisch. Frontiers in Plant Science 8:566. https://doi.org/10.3389/fpls.2017.00566

Zhang J, Zhang S, Han S, et al (2012) Genome-wide identification of microRNAs in larch and stage-specific modulation of 11 conserved microRNAs and their targets during somatic embryogenesis. Planta 236:647–657. https://doi.org/10.1007/s00425-012-1643-9

Zhang L, Fan Y, Lan Q, et al (2021a) Expression of the *SPL*-like gene *LaSPL9* in Japanese larch (*Larix leptolepis*) is regulated by *miR156* during somatic embryogenesis. Trees 35:1727–1737. https://doi.org/10.1007/s00468-020-02081-9

Zhang S, Yan S, An P, et al (2021b) Embryogenic callus induction from immature zygotic embryos and genetic transformation of *Larix kaempferi* 3× *Larix gmelinii* 9. PLoS ONE 16:e0258654. https://doi.org/10.1371/journal.pone.0258654

Zhu T, Wang J, Hu J, Ling J (2022) Mini review: application of the somatic embryogenesis technique in conifer species. Forest Research 2:18. https://doi.org/10.48130/FR-2022-0018

Xiao X, Zhang LF, Qi LW, et al (2016) Functional analysis of miR396 during somatic embryogenesis in *Larix kaempferi*. For Res 29:227–233. https://doi.org/10.13275/j.cnki.lykxyj.2016.02.012

Supplementary Files

This is a list of supplementary files associated with this preprint. Click to download.

- supplementaryfile.xlsx